Front. Optoelectron. 2021, 14(3): 360–364
https://doi.org/10.1007/s12200-020-0986-2

RESEARCH ARTICLE

Experimental Hong–Ou–Mandel interference using two independent heralded single-photon sources

Meng YE (✉), Yong WANG, Peng GAO, Likun XU, Guanjin HUANG

CSG Power Generation Company Information Communication Branch, Guangzhou 510070, China

Abstract Hong–Ou–Mandel (HOM) interference is one of the most important experimental phenomena in quantum optics. It has drawn considerable attention with respect to quantum cryptography and quantum communication because of the advent of the measurement device independent (MDI) quantum key distribution (QKD) protocol. Here, we realize HOM interference, having a visibility of approximately 38.1%, using two independent heralded single-photon sources (HSPSs). The HOM interference between two independent HSPSs is a core technology for realizing the long-distance MDI QKD protocol, the quantum coin-tossing protocol, and other quantum cryptography protocols.

Keywords Hong–Ou–Mandel (HOM), quantum cryptography, quantum key distribution (QKD)

1 Introduction

Interference plays an important role in the quantum information technology. Many quantum protocols, such as quantum cryptography [1], quantum teleportation [2], quantum repeaters [3], and quantum computing based on linear optics [4], rely upon photon interference.

The major requirement for realizing high-visibility interference is to ensure that two photons are indistinguishable in terms of all the possible degrees of freedom, including polarization, arrival time, and spectrum [5–9].

Quantum key distribution (QKD) has been an important research area in quantum information science since it was proposed in 1984 [10–16]. With the advent of quantum computing, cryptographic algorithms based on computational complexity are no longer secure; however, it has been theoretically proven that QKD attains unconditional security and can defend against quantum computing-based attacks. Regardless, the security of QKD is dependent upon its practical implementation.

To eliminate all the loopholes associated with detectors, a measurement device independent (MDI) QKD protocol was proposed [17–21]; it provides immunity against all detector attacks. MDI QKD requires high-visibility Hong–Ou–Mandel (HOM) interference. Two different optical sources can realize such interference, i.e., weak coherent states and heralded single-photon sources (HSPSs). The HOM interference between two independent weak coherent states has been studied and realized through many experiments [21,22]. It is considerably difficult to achieve HOM interference between two HSPSs because the efficiency of an HSPS based on a β–BaB_2O_2 (BBO) crystal is not sufficiently high. However, HSPSs can significantly improve the key rate of the QKD systems over long distances [23].

In this study, we present an experimental realization of HOM interference between two HSPSs. The visibility of this interference is approximately 38.1%. Our study is a step toward the realization of the long-distance MDI QKD protocol, the quantum coin-tossing protocol, and other quantum cryptography protocols.

2 Experiment

The HSPS in our experiment is based upon the spontaneous parametric down-conversion (SPDC) process in a nonlinear crystal. A BBO crystal is considered to be the nonlinear crystal. SPDC occurs when a pump photon interacting with a nonlinear medium splits into signal and idler photons. The whole process obeys the energy and momentum conservation conditions,

$$\omega_s + \omega_i = \omega_p, \tag{1}$$

$$k_s + k_i = k_p. \tag{2}$$

Received September 30, 2019; accepted December 10, 2019

E-mail: germination@126.com, yemeng@em.pgc.csg

Here, s, i and p correspond to the signal, idler, and pump photons, respectively. Further, we obtain

$$\omega_i \sin\alpha + \omega_s \sin\beta = 0, \tag{3}$$

and

$$\omega_i \cos\alpha + \omega_s \cos\beta = \frac{\omega_p n_e(\omega_p,\theta)}{n_o\left(\frac{1}{2}\omega_p\right)}, \tag{4}$$

where α and β are the phase matching angles for the signal/idler pair and θ is the cut angle of the crystal. For the degenerate condition $\omega_s = \omega_i = \frac{1}{2}\omega_p$, we have $\alpha = -\beta$. Thus, we obtain

$$\frac{1}{n_e(\omega_p,\theta)} = \frac{\sec\alpha}{n_o\left(\frac{1}{2}\omega_p\right)}. \tag{5}$$

In a nonlinear crystal, the refractive index satisfies the following equation:

$$\frac{1}{n_e(\theta)^2} = \frac{\sin^2\theta}{n_e^2} + \frac{\cos^2\theta}{n_o^2}. \tag{6}$$

Thus, we obtain

$$\frac{\sec^2\alpha}{n_o\left(\frac{1}{2}\omega_p\right)^2} = \frac{\sin^2\theta}{n_e^2} + \frac{\cos^2\theta}{n_o^2}, \tag{7}$$

where n_o and n_e can be given by the Sellmeier equation for BBO,

$$\begin{cases} n_o(\lambda)^2 = 2.7359 + \dfrac{0.01878}{\lambda^2 - 0.01822} - 0.01354\lambda^2, \\ n_e(\lambda)^2 = 2.3753 + \dfrac{0.01224}{\lambda^2 - 0.01667} - 0.01515\lambda^2, \end{cases} \tag{8}$$

where the unit of λ is μm.

Finally, we obtain a relation between the cut angle of the crystal θ and the wavelength of the pump laser,

$$\theta = \arcsin\left(\sqrt{\frac{\left(n_o\left(\frac{1}{2}\omega_p\right)\cos\alpha\right)^{-2} - n_o(\omega_p)^{-2}}{n_e(\omega_p)^{-2} - n_o(\omega_p)^{-2}}}\right). \tag{9}$$

In our experiment, the wavelength of the pump laser is 405 nm and the phase matching angle is 3.056°. We can obtain the cut angle of the BBO crystal as $\theta = 30°$ from Eq. (9).

Generally, experimental HOM interference is realized by transmitting two laser pulses to a beam splitter (BS). In practice, the splitting ratio in case of a commercial BS (free space) has an error of approximately 1%. The polarization beam splitter (PBS) in free space is better than a commercial BS (the error is approximately 0.1%). Here, we adopt an HOM interference scheme with respect to a PBS, as shown in Fig. 1. The two photons are polarized as $|H\rangle$ and $|V\rangle$. After PBS1, the two photons adopt the same path. Thus, the quantum state can be given as

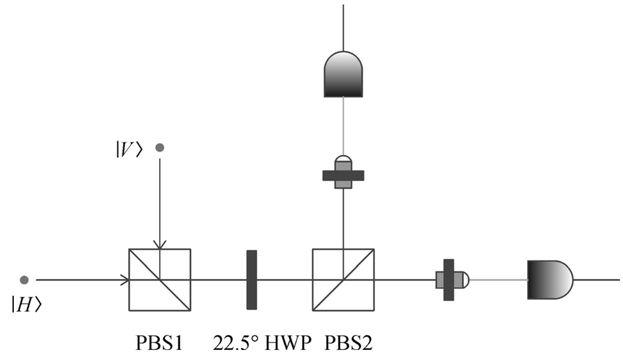

Fig. 1 An HOM interference scheme containing two PBSs. The two photons are polarized as $|H\rangle$ and $|V\rangle$. PBS, polarization beam splitter; HWP, half-wave plate

$$\hat{a}_H^\dagger \hat{a}_V^\dagger |0\rangle. \tag{10}$$

After the half-wave plate observed at 22.5°, the quantum state is

$$\frac{1}{\sqrt{2}}\left(\hat{a}_H^\dagger + \hat{a}_V^\dagger\right) \otimes \frac{1}{\sqrt{2}}\left(\hat{a}_H^\dagger - \hat{a}_V^\dagger\right)|0\rangle$$

$$= \frac{1}{2}\left(\hat{a}_H^\dagger \hat{a}_H^\dagger - \hat{a}_V^\dagger \hat{a}_V^\dagger\right)|0\rangle = \frac{1}{\sqrt{2}}(|2\rangle_H - |2\rangle_V). \tag{11}$$

From Eq. (11), the two photons are observed to bunch together, which denotes the HOM interference.

The overall light path diagram is shown in Fig. 2. Our experiment was implemented using two HSPSs. A pulse train from a mode-locked Ti:sapphire laser (with a duration of 2.5 ps, a repetition rate of 76 MHz, and a central wavelength of 780 nm) was passed through a frequency doubler (LiB_3O_5 (LBO) crystal). Subsequently, the 390-nm pulse laser from the frequency doubler pumped the BBO crystal having a thickness of 0.3 mm. With the progress of type-I SPDC, two 780-nm photons will be emitted from the BBO crystal. One photon was directly coupled into a 780-nm single-mode fiber (SMF) and detected using a single-photon counting module (SPD), with a detection efficiency of approximately 62% at 780 nm as a heralded photon. The other photon (a signal photon) is coupled to the SMF and emitted by a fiber collimator. The full width at half maxima (FWHM) bandwidth of the band pass interference filter is 3.0 nm.

To compensate for the alteration of polarization by SMF, we put two half-wave plates (780 nm) into the light's path, i.e., one in front of the fiber coupler (H1) and the other (H2) behind the fiber emitter (both the fiber coupler and fiber emitter are fiber collimators, F220FC-780, from Thorlabs, Inc., USA). Because SMF is altered by the birefringence effect, we treat the SMF as a wave plate. H1 rotates the linear polarization of the signal photon to ensure agreement with the optical axis of the SMF, such that the polarization of the signal photon remains linear after emission from the fiber collimator. H2 rotates the polarization of the signal photon into the original state.

Two HSPSs are realized using the same scheme containing BBO1 and BBO2 in Fig. 2. To realize high-visibility HOM interference, it is critical to ensure that the two photons are indistinguishable in terms of all possible degrees of freedom, including polarization, arrival time, and frequency. The PBS after H2 ensures that the polarizations of the signal photons from the two BBOs are vertical. After PBS, the bandpass interference filter (BPIF) filters the two photons to ensure that their spectrums are identical. The motorized positioning systems are used to scan the arrival times of the two photons.

The experimental result is shown in Fig. 3, where "2-fold" indicates the coincidence count between SPD3 and SPD4. The coincidence window is 2 ns. "4-fold" indicates the coincidence count between SPD1, SPD2, SPD3, and SPD4. The average 4-fold count is approximately 10 c/min, indicating that the experimental period is considerably long. To eliminate the influence of instability with respect to experimental factors (including the power of the laser and the temperature of the laboratory), data normalization is demonstrated. Finally, a dip can be observed when the interference visibility is 38.1% in our experiment, indicating that HOM interference can be realized using two independent HSPSs.

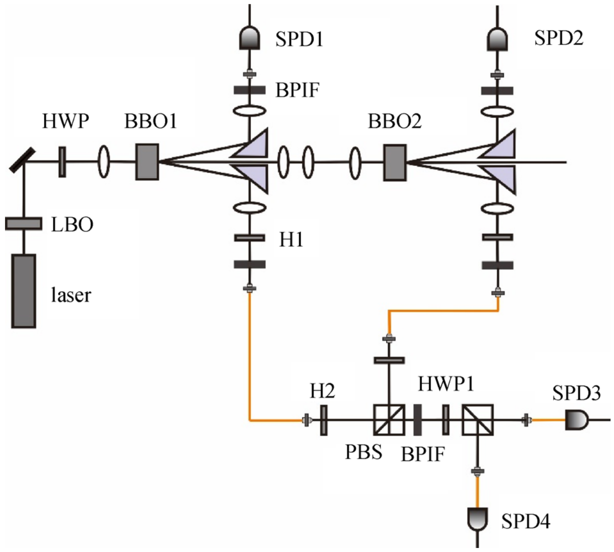

Fig. 2 Setup of HOM interference experiment. HWP, half-wave plate; LBO, LiB_3O_5; BBO, β–BaB_2O_2; BPIF, bandpass interference filter; H1, H2, half-wave plates for polarization compensation; PBS, polarization beam splitter; SPD, single-photon detector

3 Discussion and conclusion

Thus, HOM interference was realized between two independent HSPSs. The HOM interference visibility is approximately 38.1%. As shown in Ref. [24], the visibility of the two independent photons is mainly determined by

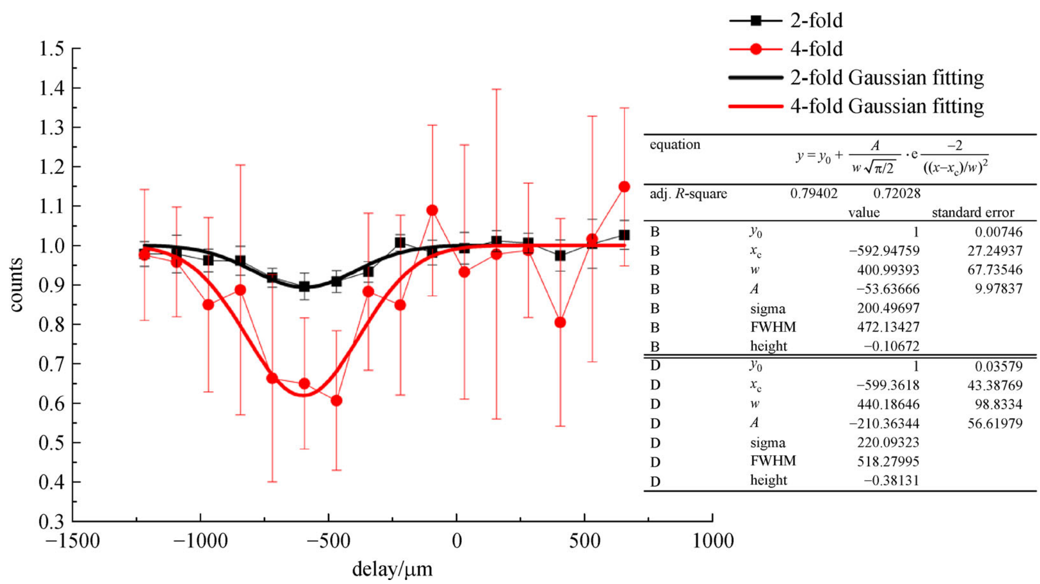

Fig. 3 HOM dip in our experiment. The solid line denotes the Gaussian fitting. B represents the black fit curve and D represents the red fit curve in the figure. The fitting formula y is a Gaussian fitting function. A and w are parameters in the formula

their indistinguishability. The time uncertainties of the two photons must be considerably smaller than their coherent times; this relation can be simply expressed by stating that the greater the coincidence between the time wave packets of the two interferometry photons, the higher will be the interference visibility. This visibility is determined based on the pulse width of the pump laser and the coherence time of the signal photons as [24]

$$V = 1/\sqrt{1 + \left(\frac{\Delta T}{\tau}\right)^2}, \tag{12}$$

where ΔT is the pulse width of the pump laser and τ is the coherence time of the signal photons, which is determined using the BPIF in our experiment, where the pulse width of the pump laser is approximately 2.5 ps. The bandwidth of the BPIF is approximately 3 nm. If we use a filter with a narrow bandwidth or select a pump laser with a narrow pulse width (100 fs is available), the visibility can be improved to become more than 99%.

Our study is a step toward the realization of the long-distance MDI QKD protocol, the quantum coin-tossing protocol, and other quantum cryptography protocols.

References

1. Gisin N, Ribordy G, Tittel W, Zbinden H. Quantum cryptography. Reviews of Modern Physics, 2002, 74(1): 145–195
2. Bouwmeester D, Pan J W, Mattle K, Eibl M, Weinfurter H, Zeilinger A. Experimental quantum teleportation. Nature, 1997, 390(6660): 575–579
3. Briegel H J, Dür W, Cirac J I, Zoller P. Quantum repeaters: the role of imperfect local operations in quantum communication. Physical Review Letters, 1998, 81(26): 5932–5935
4. Knill E, Laflamme R, Milburn G J. A scheme for efficient quantum computation with linear optics. Nature, 2001, 409(6816): 46–52
5. Hong C K, Ou Z Y, Mandel L. Measurement of subpicosecond time intervals between two photons by interference. Physical Review Letters, 1987, 59(18): 2044–2046
6. Rarity J G, Tapster P R, Loudon R. Non-classical interference between independent sources. Journal of Optics B: Quantum and Semiclassical Optics, 2005, 7(7): S171–S175
7. Kaltenbaek R, Blauensteiner B, Zukowski M, Aspelmeyer M, Zeilinger A. Experimental interference of independent photons. Physical Review Letters, 2006, 96(24): 240502
8. Beugnon J, Jones M P, Dingjan J, Darquié B, Messin G, Browaeys A, Grangier P. Quantum interference between two single photons emitted by independently trapped atoms. Nature, 2006, 440(7085): 779–782
9. Bennett A J, Patel R B, Nicoll C A, Ritchie D A, Shields A J. Interference of dissimilar photon sources. Nature Physics, 2009, 5 (10): 715–717
10. Bennet C H, Brassard G. Quantum Cryptography: Public-Key Distribution and Tossing. In: Proceedings of IEEE International Conference on Computers, Systems and Signal Processing. Bangalore: IEEE Press, 1984, 175–179
11. Zhang C M, Li M, Huang J Z, Li H W, Li F Y, Wang C, Yin Z Q, Chen W, Han Z F, Treeviriyanupab P, Sripimanwat K. Fast implementation of length-adaptive privacy amplification in quantum key distribution. Chinese Physics B, 2014, 23(9): 090310
12. Zhang C M, Song X T, Treeviriyanupab P, Li M, Wang C, Li H W, Yin Z Q, Chen W, Han Z F. Delayed error verification in quantum key distribution. Chinese Science Bulletin, 2014, 59(23): 2825–2828
13. Li M, Patcharapong T, Zhang C M, Yin Z Q, Chen W, Han Z F. Efficient error estimation in quantum key distribution. Chinese Physics B, 2015, 24(1): 010302
14. Wang S, He D Y, Yin Z Q, Lu F Y, Cui C H, Chen W, Zhou Z, Guo G C, Han Z F. Beating the fundamental rate-distance limit in a proof-of-principle quantum key distribution system. Physical Review X, 2019, 9(2): 021046
15. Li Y P, Chen W, Wang F X, Yin Z Q, Zhang L, Liu H, Wang S, He D Y, Zhou Z, Guo G C, Han Z F. Experimental realization of a reference-frame-independent decoy BB84 quantum key distribution based on Sagnac interferometer. Optics Letters, 2019, 44(18): 4523–4526
16. Lu F Y, Yin Z Q, Cui C H, Fan-Yuan G J, Wang R, Wang S, Chen W, He D Y, Huang W, Xu B J, Guo G C, Han Z F. Improving the performance of twin-field quantum key distribution. Physical Review A, 2019, 100(2): 022306
17. Lo H K, Curty M, Qi B. Measurement-device-independent quantum key distribution. Physical Review Letters, 2012, 108(13): 130503
18. Ferreira da Silva T, Vitoreti D, Xavier G B, do Amaral G C, Temporão G P, von der Weid J P. Proof-of-principle demonstration of measurement-device-independent quantum key distribution using polarization qubits. Physical Review A, 2013, 88(5): 052303
19. Rubenok A, Slater J A, Chan P, Lucio-Martinez I, Tittel W. Real-world two-photon interference and proof-of-principle quantum key distribution immune to detector attacks. Physical Review Letters, 2013, 111(13): 130501
20. Liu Y, Chen T Y, Wang L J, Liang H, Shentu G L, Wang J, Cui K, Yin H L, Liu N L, Li L, Ma X, Pelc J S, Fejer M M, Peng C Z, Zhang Q, Pan J W. Experimental measurement-device-independent quantum key distribution. Physical Review Letters, 2013, 111(13): 130502
21. Tang Z, Liao Z, Xu F, Qi B, Qian L, Lo H K. Experimental demonstration of polarization encoding measurement-device-independent quantum key distribution. Physical Review Letters, 2014, 112(19): 190503
22. Chen H, An X B, Wu J, Yin Z Q, Wang S, Chen W, Han Z F. Hong–Ou–Mandel interference with two independent weak coherent states. Chinese Physics B, 2016, 25(2): 020305
23. Wang Q, Chen W, Xavier G, Swillo M, Zhang T, Sauge S, Tengner M, Han Z F, Guo G C, Karlsson A. Experimental decoy-state quantum key distribution with a sub-poissionian heralded single-photon source. Physical Review Letters, 2008, 100(9): 090501
24. Zukowski M, Zeilinger A, Weinfurter H. Entangling photons radiated by independent pulsed sourcesa. Annals of the New York Academy of Sciences, 1995, 755(1): 91–102

Meng Ye earned his master's degree in electronic and information engineering from South China University of Technology, China. Currently, he is the vice chief engineer of the Power Generation Company, China and a director of its communications department. His research interests include optical transmission and communications technology management.

E-mail: gexmination@126.com, yemeng@em.pgc.csg

Yong Wang is a senior engineer at the Power Generation Company, China. His research mainly focuses on enterprise communication system management, technological innovation, and operations.

E-mail: wangyong@em.pgc.csg

Peng Gao earned his master's degree in communications engineering from South China University of Technology, China. Currently, he is a senior engineer at the China Southern Power Grid Co., Ltd., China. Recently, his research has focused on network security, wireless communications, and power-line communications.

E-mail: gaopeng@em.pgc.csg

Likun Xu is an engineer at the Power Generation Company, China. His research focuses on smart grids and operations management of information systems in the electric power industry.

E-mail: xlk@em.pgc.csg

Guanjin Huang earned his master's degree in electronics and information engineering from South China University of Technology, China. Currently, he is a senior engineer at the Power Generation Company, China. His research interests include network security, wireless communications, and power-line communications.

E-mail: huanggj@em.pgc.csg